**Article:**
Bevan, T., Hornsby, J., Merabet, N. et al. (2018) A biomechanical model for fibril recruitment: Evaluation in tendons and arteries. Journal of Biomechanics, 74. pp. 192-196. ISSN: 0021-9290

https://doi.org/10.1016/j.jbiomech.2018.03.047

# A biomechanical model for fibril recruitment: evaluation in tendons and arteries

Tim Bevan[1], Nadege Merabet[1], Jack Hornsby[1], Paul N Watton[2,3], Mark S Thompson[1]

1. Institute of Biomedical Engineering, University of Oxford, United Kingdom

2. Department of Computer Science & INSIGNEO Institute for In Silico Medicine, University of Sheffield, United Kingdom

3. Mechanical Engineering and Materials Science, University of Pittsburgh, US

Submit to J Biomech, short communication
Version 5. 14/02/2018

Corresponding author:

Dr. Mark S. Thompson

Institute of Biomedical Engineering,

University of Oxford,

Botnar Research Centre,

Oxford OX3 7LD.

UK

Telephone: +44 1865 737845

Fax: +44 1865 737640

Email: mark.thompson@eng.ox.ac.uk

Keywords: Tendon; artery; mechanobiology; fibril recruitment; collagen

## Abstract

Simulations of soft tissue mechanobiological behaviour are increasingly important for clinical prediction of aneurysm, tendinopathy and other disorders. Mechanical behaviour at low stretches is governed by fibril straightening, transitioning into load-bearing at recruitment stretch, resulting in a tissue stiffening effect. Previous investigations have suggested theoretical relationships between stress-stretch measurements and recruitment probability density function (PDF) but not derived these rigorously nor evaluated these experimentally. Other work has proposed image-based methods for measurement of recruitment but made use of arbitrary fibril critical straightness parameters. The aim of this work was to provide a sound theoretical basis for estimating recruitment PDF from stress-stretch measurements and to evaluate this relationship using image-based methods, clearly motivating the choice of fibril critical straightness parameter in rat tail tendon and porcine artery. Rigorous derivation showed that the recruitment PDF may be estimated from the second stretch derivative of the first Piola-Kirchoff tissue stress. Image-based fibril recruitment identified the fibril straightness parameter that maximised Pearson correlation coefficients (PCC) with estimated PDFs. Using these critical straightness parameters the new method for estimating recruitment PDF showed a PCC with image-based measures of 0.915 and 0.933 for tendons and arteries respectively. This method may be used for accurate estimation of fibril recruitment PDF in mechanobiological simulation where fibril-level mechanical parameters are important for predicting cell behaviour.

## Introduction

The complex microstructural arrangement of collagen and elastin fibrils endows highly loaded soft tissues such as blood vessels and tendons with their unique mechanical properties. These fibrils commonly have high tortuosity ("crimp") at low stretches which is removed as the tissue stretch is increased, resulting in a stiffening behaviour as observed with in situ loading experiments using multiple imaging modalities: Atomic Force Microscopy (AFM) (Rigozzi et al., 2011), Optical Coherence Tomography (OCT) (Hansen et al., 2002), X-ray scattering (Fratzl et al., 1998), polarizing microscopy (Diamant et al., 1972). As each fibril uncrimps at its recruitment stretch it begins to bear load, so the distribution of recruitment stretches for a tissue is an important determinant of the tissue mechanical property.

The recruitment stretch plays a significant role in the static and dynamic fatigue properties of these tissues – more highly loaded fibrils may fail first (Fung et al., 2009). Recruitment is also important in the mechanobiology of the tissue, as the local mechanical environment for mechanosensitive cells is profoundly altered with fibril uncrimping (Hill et al., 2012; Watton et al., 2004; Wren et al., 1998) and modulating cell behaviour through extracellular matrix stiffness is proposed as a novel target for multiple diseases (Lampi and Reinhart-King, 2018).

Many constitutive material models for fibrillar soft tissues have been proposed, either phenomenologically representing the tissue stiffening effect of recruitment (Fung, 1967; Holzapfel et al., 2000) or explicitly representing fibril recruitment with a distribution of recruitment stretches (Frisén et al., 1969). A variety of different probability distribution functions (PDF) for recruitment have been proposed and fitted to experimental data (Hill et al., 2012). The simplest, a triangular PDF has three parameters (start of recruitment, maximum rate of recruitment, end of recruitment) that are readily identifiable from imaging data (Aparicio et al., 2016).

Direct measurement of fibril recruitment from microscopy has used the concept of straightness ratio, $S$ and a critical value, $S_c$ such that a fibril may be considered to be load bearing if $S > S_c$. Various different values for $S_c$ have been used, apparently arbitrarily.

It has been proposed that the second derivative of the stress stretch relationship is proportional to the fibril recruitment PDF (Bontempi, 2009) but without rigorous derivation and evaluation against imaging data of fibril recruitment. The aims of this work were to provide a rigorous proof of the fibril recruitment stretch PDF relationship to the second derivative of stress with respect to stretch, to evaluate this relationship experimentally in rat tail tendons and porcine arteries and explore its sensitivity to critical straightness ratios. The hypothesis was that the stress stretch derivative parameter was correlated to image-based measures of the recruitment PDF. In situ microscopy was used to obtain measures of fibril recruitment and stress stretch behaviour in the same specimen under tensile load. Tendon and artery were chosen as having both strong clinical and scientific interest and widely differing stress-stretch behaviour to test this relationship.

## Materials and methods

*Theoretical development*

We use the term fibril to refer to a quasi-crystalline filament of collagen 50 – 500 nm in diameter, as defined for tendon (Handsfield et al., 2016). Let the macroscale tissue stretch of a fibrillar tissue undergoing a tensile test be $\lambda = 1 + e$ where $e$ is engineering strain. Both are $\lambda$ and $e$ are work conjugate to the first Piola-Kirchhoff stress. Any individual fibril bears no load until $\lambda = \lambda_R$, where $\lambda_R$ is the recruitment stretch for that fibril. The macroscale tissue strain energy density function $W_t(\lambda)$ is the integral of the energies of individual fibrils $W_f(\lambda, \lambda_R)$ over all recruitment stretches $\lambda_R \leq \lambda$ weighted by the probability density function $g(\lambda_R)$ that an individual fibril has a given recruitment stretch $\lambda_R$. Using rule of mixtures and assuming tensile load is carried only by one family of fibrils, we include the fibril area fraction $\phi$ for this family. This gives:

$$W_t(\lambda) = \phi \int_1^{\lambda} g(\lambda_R)\, W_f(\lambda, \lambda_R)\, d\lambda_R$$

We choose a simple strain energy function (SEF) for a fibril (Hill et al., 2012) using $\lambda_f = \lambda/\lambda_R$ as the fibril stretch:

$$W_f = E\frac{\left(\lambda_f - 1\right)^2}{2} = E\frac{(\lambda - \lambda_R)^2}{2\lambda_R^2}$$

so the whole tissue SEF is

$$W_t(\lambda) = \phi E \int_1^{\lambda} g(\lambda_R)\ \frac{(\lambda - \lambda_R)^2}{2\lambda_R^2}\ d\lambda_R$$

where $E$ is the elastic modulus of a fibril, assumed constant for all fibrils.

The first Piola-Kirchhoff whole tissue stress, $P_t$, is given:

$$P_t = \frac{dW_t}{de} = \frac{dW_t}{d\lambda}\frac{d\lambda}{de} = \frac{d}{d\lambda}\left[\phi E \int_1^{\lambda} g(\lambda_R)\ \frac{(\lambda - \lambda_R)^2}{2\lambda_R^2}\ d\lambda_R\right]$$

This can be simplified using the Leibniz integral rule, which has standard form as follows (Protter and Morrey, 1985):

$$\frac{d}{d\lambda}\left[\int_{a(\lambda)}^{b(\lambda)} f(\lambda, \lambda_R) d\lambda_R\right] = f\big(\lambda, b(\lambda)\big)\frac{db}{d\lambda} - f\big(\lambda, a(\lambda)\big)\frac{da}{d\lambda} + \int_{a(\lambda)}^{b(\lambda)} f_\lambda(\lambda, \lambda_R)\ d\lambda_R$$

Here we set $f(\lambda, \lambda_R) = g(\lambda_R)\ (\lambda - \lambda_R)^2/2\lambda_R^2$ and confirm that $f(\lambda, \lambda_R)$ and $f_\lambda$, its partial derivative with respect to $\lambda$, are continuous in the domain of interest, and the integral limits $a(\lambda) = 1$ and $b(\lambda) = \lambda$ and their derivatives with respect to $\lambda$ are also continuous in this domain.

Therefore we obtain

$$P_t = \phi E \int_1^{\lambda} g(\lambda_R)\frac{(\lambda - \lambda_R)}{\lambda_R^2}\ d\lambda_R$$

applying the rule a second time with the same continuity assumptions gives

$$\frac{dP_t}{d\lambda} = \phi E \int_1^{\lambda} g(\lambda_R)\frac{1}{\lambda_R^2}\ d\lambda_R$$

and applying a third time:

$$\frac{d^2P_t}{d\lambda^2} = \phi E\, g(\lambda)\frac{1}{\lambda^2}$$

This motivates the definition of a stress stretch parameter, $\zeta = \lambda^2 \frac{d^2P_t}{d\lambda^2} = \phi E\, g(\lambda)$ with units of Pa, to estimate the recruitment stretch PDF $g(\lambda)$ from mechanical tests.

*Experimental work*

Rat tail tendon fascicles (n=7) were collected from 10-week old rats sacrificed in unrelated work. Tendon fascicles were dissected from the distal end of each tail. The mean cross-sectional area of each specimen assuming circularity was calculated from three optical micrometer (Keyence, Milton Keynes, UK; precision $10^{-5}$ mm) measurements of diameter under a tare load of 0.05 N. Samples were stored at -20°C for up to one week before use. Prior to imaging and testing samples were removed from the freezer and allowed to warm in phosphate buffered saline (PBS) to room temperature for two hours.

Porcine aortic arteries (n=5) were dissected within an hour of sacrifice from 6 month old Landrace pigs' hearts obtained from a local abattoir. Samples from the aortic arch region were carefully excised, cut longitudinally and then into circumferential strips. Width and height dimensions of samples were obtained as an average of three measurements again using an optical micrometer under a tare load of 0.05 N. Samples were then stored in phosphate buffer solution (PBS) at -20°C for over 24 hours. Prior to imaging and testing samples were removed from the freezer and allowed to warm to room temperature for two hours.

Mechanical testing was carried out using a custom-built uniaxial micro-tensile testing machine (linear actuator resolution 1 μm, T–NA0A850, Zaber; load cell resolution 0.033 N, WMC–5, Interface). The tissue was held in custom clamps and suspended in a PBS bath on a 0.13 mm thick glass cover slip over the inverted microscope objective. The artery strips were extended in the circumferential direction. Zero strain was defined with a tare load of 50 mN. A mean stress-strain curve was obtained for each specimen from four displacement ramp loadings at 0.2% $s^{-1}$ to 4% (tendon) or 100% (artery) strain, data sampled at 10 Hz with 5 minutes rest between each test. The

second derivatives of the stress-stretch curves for each tissue sample were obtained using cubic spline fits and numerical differentiation in Matlab.

The testing machine was mounted on an LSM 710 inverted confocal laser-scanning microscope (Zeiss, UK) fitted with a tunable pulsed femtosecond titanium-sapphire Chameleon laser (Coherent, UK) operating at 860 nm. SHG signal was collected at 430 nm. A stepped displacement protocol with increments of 0.5% strain (tendon) or 7% strain (artery) was used to apply up to 4% strain (tendon) or 100% (artery). After a 2 minute equilibration time at each step, a z-stack comprising six images at 20 μm z-intervals of the SHG signal was acquired up to a depth of 100 μm in the tissue. Fibrils were traced semi-automatically using NeuronJ 1.4.3 (Meijering et al., 2004) in each image at each stretch. The algorithm was guided by hand so that only fibrils that appeared at all stretch levels were assessed and it was found that six fibrils per image, giving 36 per z-stack, could be reliably identified (Fig 1). The straightness ratio, $S$, was calculated for each fibril (Hill et al., 2012):

$$S = \frac{L_{chord}}{L_{spline}}$$

where $L_{chord}$ is the point to point distance and $L_{spline}$ the length along the fibril path. The critical straightness ratio $S_c$, defines the straightness at which a fibril may be considered to be recruited into load bearing. This study investigated $0.980 < S_c < 0.995$ in steps of 0.0025 covering the range of values previously reported (Hill et al., 2012; Roy et al., 2011).

*Image-based vs stress based recruitment profiles*

For each value of $S_c$ a least squares best fit was found for the image measured fibril recruitment distribution using a triangular PDF via the related piece-wise quadratic cumulative density function (CDF). The Pearson correlation coefficient (PCC) was calculated between the measured PDFs and the stress-stretch parameter $\zeta$. The value of $S_c$ that maximised PCC was denoted $S_c^*$. Differences between tissues were assessed using a two-tailed Mann Whitney test due to small sample sizes with significance set to $p<0.05$.

## Results

Qualitatively similar curve shapes were found for the stress-stretch second derivative and image-based recruitment PDF in both tendon (Fig 2) and artery (Fig 3).

There was strong sensitivity of the PCC on $S_c$ (Fig 4) with a clear peak in the relationship.

The mean value (standard deviation) of $S_c^*$, the critical straightness ratio that maximised the PCC for rat tail tendons (n=7) was 0.991 (0.003), while for porcine artery (n=5) this was 0.996 (0.0007). For comparison, the straightness ratios $S$ in unloaded tissue were 0.9842 (0.009) in tendon and 0.9620 (0.0170) in artery. Post-hoc testing showed a significant difference in $S_c^*$ between tendon and artery. Using the mean values of $S_c^*$, the obtained PCC between the stress stretch parameter and image-based PDF was 0.915 (0.030) and 0.933 (0.041) for tendons and arteries respectively.

## Discussion

We report a rigorous derivation of the relationship between uniaxial stress-stretch behaviour and fibril recruitment PDF together with a positive evaluation of this relationship in tendon and artery. The mean Pearson's correlation coefficients for the stress-stretch derived parameters with image-based fibril recruitment PDFs were over 0.9. This supports the use of uniaxial mechanical tests in probing the microstructural arrangement of fibre composite materials.

The strength of the correlations was highly sensitive to the arbitrarily chosen critical straightness ratio with a clear peak, motivating the definition of $S_c^*$, the critical straightness ratio for maximum correlation. The critical straightness ratio for any given fibril will likely depend upon the ratio of fibril bending to axial stiffness. Assuming homogeneous fibrils and simple beam theory this ratio is given by the second moment of area of the fibril, so that thicker fibrils will have a smaller $S_c^*$. The larger $S_c^*$ in the artery samples may therefore suggest a recruitment process of smaller diameter fibrillar units compared with the tendon samples. Collagen fibril diameter is known to depend upon species, age and anatomical site however there are indications that fibrils in porcine arteries may be smaller than those in rat tail tendons. (Merrilees et al., 1987; Parry et al., 1978).

Previous work developed a similar relationship without rigorous proof and provided limited evaluation based on data provided by other authors (Bontempi, 2009). Previous authors suggested arbitrary values for the critical straightness at which a fibre could be considered to be load bearing (Hill et al., 2012; Roy et al., 2011). We have shown the high sensitivity of the recruitment model to this parameter and suggested one way of determining it.

There are several limitations to this study. Firstly the recruitment in only one dimension under uniaxial load is described, which is physiologically relevant for uniaxial tissues such as tendons. The present theory does not extend to general biaxial loading since the complex non-affine behaviour of the fibrils is not represented. The non-physiological loading of artery which also disregards residual stresses and other load bearing components including elastin may nevertheless provide useful information on the tissue microstructure. Also, a linear fibril stretch to stress relation is assumed, whereas non-linear behaviour is observed with single fibril testing at strains of up to 4% (van der Rijt et al., 2006). It would be straightforward to include fibril non-linearity, but the required numerical integration would obscure the simple relationships highlighted by the analytical formulation presented here. Fibril straightness was measured following a 2 minute relaxation time allowed between each load step and image acquisition, while the stress-stretch data was obtained during a continuous 0.2% $s^{-1}$ ramp. Only a small number of specimens from two different tissues have been used to evaluate the relationship. The relationship should be confirmed in more specimens from other relevant tissues.

In conclusion we report a new, rigorous derivation of a relationship between macroscopically measurable mechanical parameters and microstructural fibril recruitment and show positive evaluations in two widely different tissues. This relationship may be used in future to extract recruitment distributions directly from stress-stretch behaviour of fibrous materials for the purpose of accurate modelling of the tissue mechanobiological environment.

## Acknowledgements

Rosetrees Trust (M186-F1) are acknowledged for their generous support of this project. Jack

Hornsby's studentship was supported by the RCUK Digital Economy Programme grant number EP/G036861/1 (Oxford Centre for Doctoral Training in Healthcare Innovation). We would like to thank Dr. Clarence Yapp (University of Oxford, UK) for providing microscope training and expertise.

## References

Aparicio, P., Thompson, M.S., Watton, P.N., 2016. A novel chemo-mechano-biological model of arterial tissue growth and remodelling. J Biomech 49, 2321-2330.

Bontempi, M., 2009. Probabilistic model of ligaments and tendons: quasistatic linear stretching. Phys Rev E Stat Nonlin Soft Matter Phys 79, 030903.

Diamant, J., Keller, A., Baer, E., Litt, M., Arridge, R.G.C., 1972. Collagen ultrastructure and its relation to mechanical properties as a function of ageing. Proceedings of the Royal Society of London. Series B: Biological Sciences 180, 293-315.

Fratzl, P., Misof, K., Zizak, I., Rapp, G., Amenitsch, H., Bernstorff, S., 1998. Fibrillar structure and mechanical properties of collagen. J Struct Biol 122, 119-122.

Frisén, M., Mägi, M., Sonnerup, L., Viidik, A., 1969. Rheological analysis of soft collagenous tissue Part I: Theoretical considerations. Journal of Biomechanics 2, 13-20.

Fung, D.T., Wang, V.M., Laudier, D.M., Shine, J.H., Basta-Pljakic, J., Jepsen, K.J., Schaffler, M.B., Flatow, E.L., 2009. Subrupture tendon fatigue damage. Journal of Orthopaedic Research 27, 264-273.

Fung, Y.C., 1967. Elasticity of soft tissues in simple elongation. American Journal of Physiology 213, 1532-1544.

Handsfield, G.G., Slane, L.C., Screen, H.R., 2016. Nomenclature of the tendon hierarchy: An overview of inconsistent terminology and a proposed size-based naming scheme with terminology for multi-muscle tendons. J Biomech 49, 3122-3124.

Hansen, K.A., Weiss, J.A., Barton, J.K., 2002. Recruitment of tendon crimp with applied strain. Journal of Biomechanical Engineering 124, 72-77.

Hill, M.R., Duan, X., Gibson, G.A., Watkins, S., Robertson, A.M., 2012. A theoretical and non-destructive experimental approach for direct inclusion of measured collagen orientation and recruitment into mechanical models of the artery wall. J Biomech 45, 762-771.

Holzapfel, G., Gasser, T.C., Ogden, R.W., 2000. A new constitutive framework for arterial wall mechanics and a comparative study of material models. Journal of Elasticity 61, 1-48.

Lampi, M.C., Reinhart-King, C.A., 2018. Targeting extracellular matrix stiffness to attenuate disease: From molecular mechanisms to clinical trials. Sci Transl Med 10.

Meijering, E., Jacob, M., Sarria, J.C.F., Steiner, P., Hirling, H., Unser, M., 2004. Design and Validation of a Tool for Neurite Tracing and Analysis in Fluorescence Microscopy Images. Cytometry 58A, 167-176.

Merrilees, M.J., Tiang, K.M., Scott, L., 1987. Changes in collagen fibril diameters across artery walls including a correlation with glycosaminoglycan content. Connect Tissue Res 16, 237-257.

Parry, D.A., Barnes, G.R., Craig, A.S., 1978. A comparison of the size distribution of collagen fibrils in connective tissues as a function of age and a possible relation between fibril size distribution and mechanical properties. Proc R Soc Lond B Biol Sci 203, 305-321.

Protter, M.H., Morrey, C.B., 1985. Differentiation under the Integral Sign, Intermediate Calculus. Springer, New York, pp. 421-426.

Rigozzi, S., Stemmer, A., Muller, R., Snedeker, J.G., 2011. Mechanical response of individual collagen fibrils in loaded tendon as measured by atomic force microscopy. J Struct Biol 176, 9-15.

Roy, S., Boss, C., Rezakhaniha, R., Stergiopulos, N., 2011. Experimental characterization of the distribution of collagen fiber recruitment. Journal of Biorheology 24, 84-93.

van der Rijt, J.A., van der Werf, K.O., Bennink, M.L., Dijkstra, P.J., Feijen, J., 2006. Micromechanical testing of individual collagen fibrils. Macromolecular bioscience 6, 697-702.

Watton, P.N., Hill, N.A., Heil, M., 2004. A mathematical model for the growth of the abdominal aortic aneurysm. Biomech Model Mechanobiol 3, 98-113.

Wren, T.A., Beaupre, G.S., Carter, D.R., 1998. A model for loading-dependent growth, development, and adaptation of tendons and ligaments. J Biomech 31, 107-114.

**Figure 1**
Click here to download Figure: Fig1_v5.docx

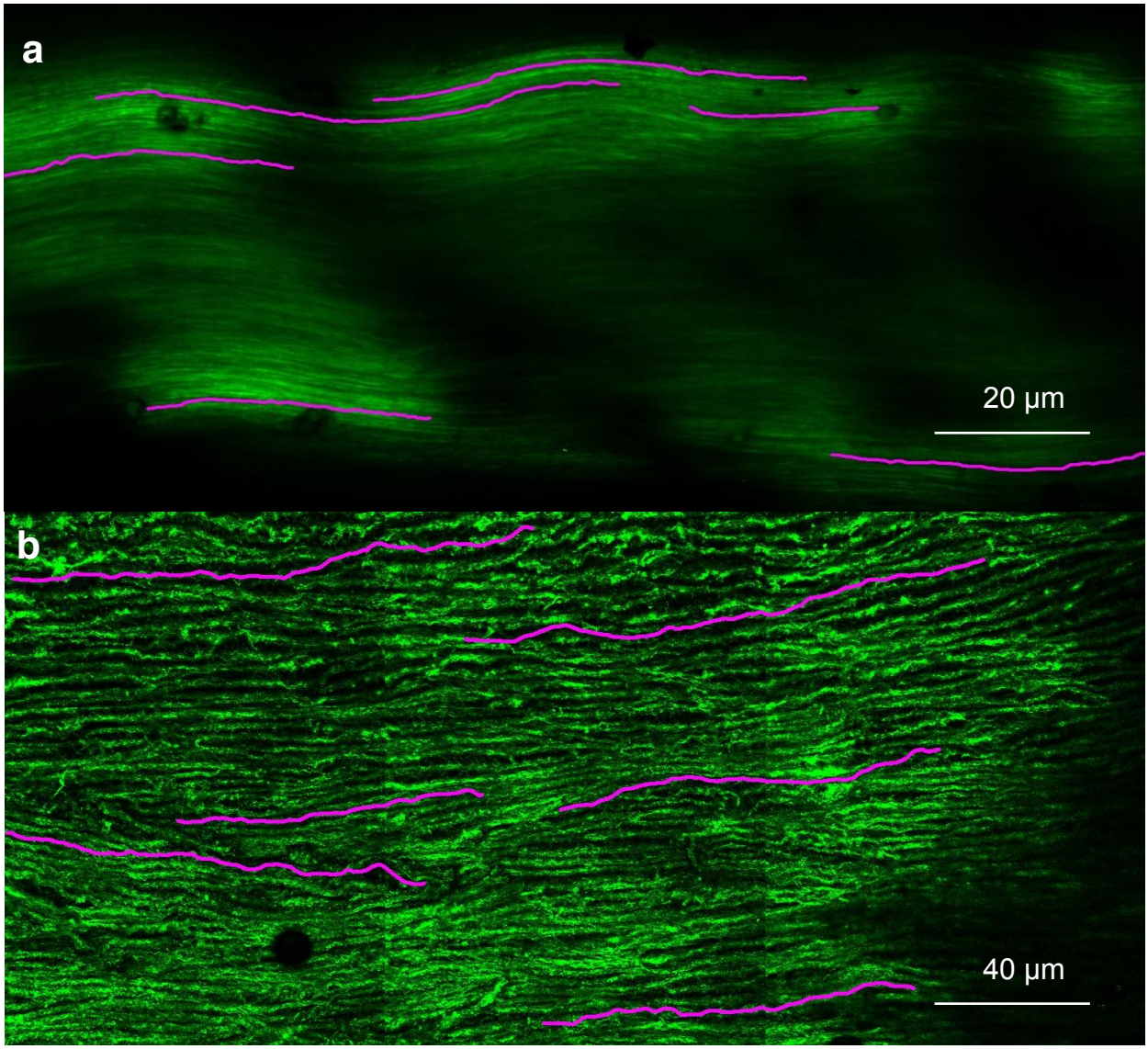


**Figure 1.a** Unloaded tendon and **b** artery collagen fibrils SHG signal (green) with NeuronJ fibril traces (purple) superimposed.

**Figure 2**
**Click here to download Figure: Fig2_v5.docx**

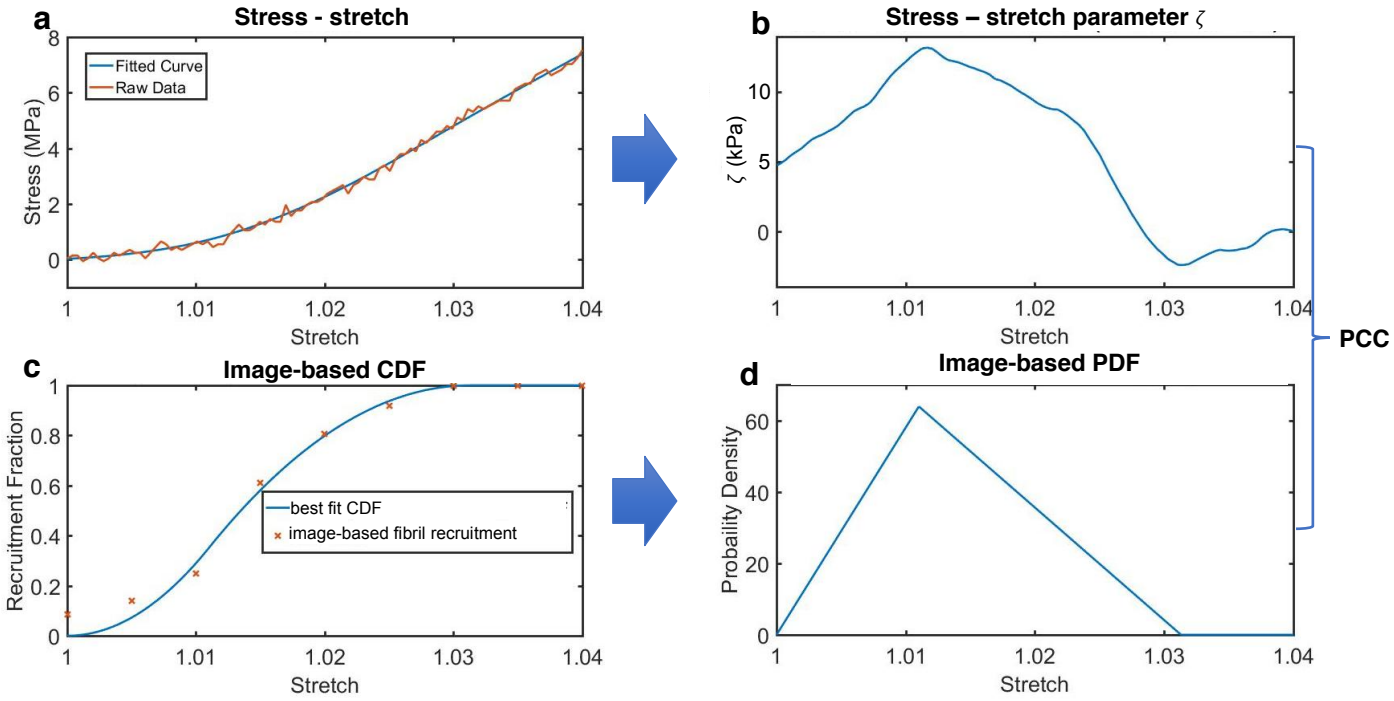


**Figure 2.a** Exemplary tendon stress-stretch curve, spline fitted. **b** Stress-stretch parameter $\zeta$. **c** Image-based fibril recruitment and best-fit CDF for $S_c = S_c^*$. **d** corresponding PDF. PCC calculated for **b** compared with **d**

**Figure 3**
**Click here to download Figure: Fig3_v5.docx**

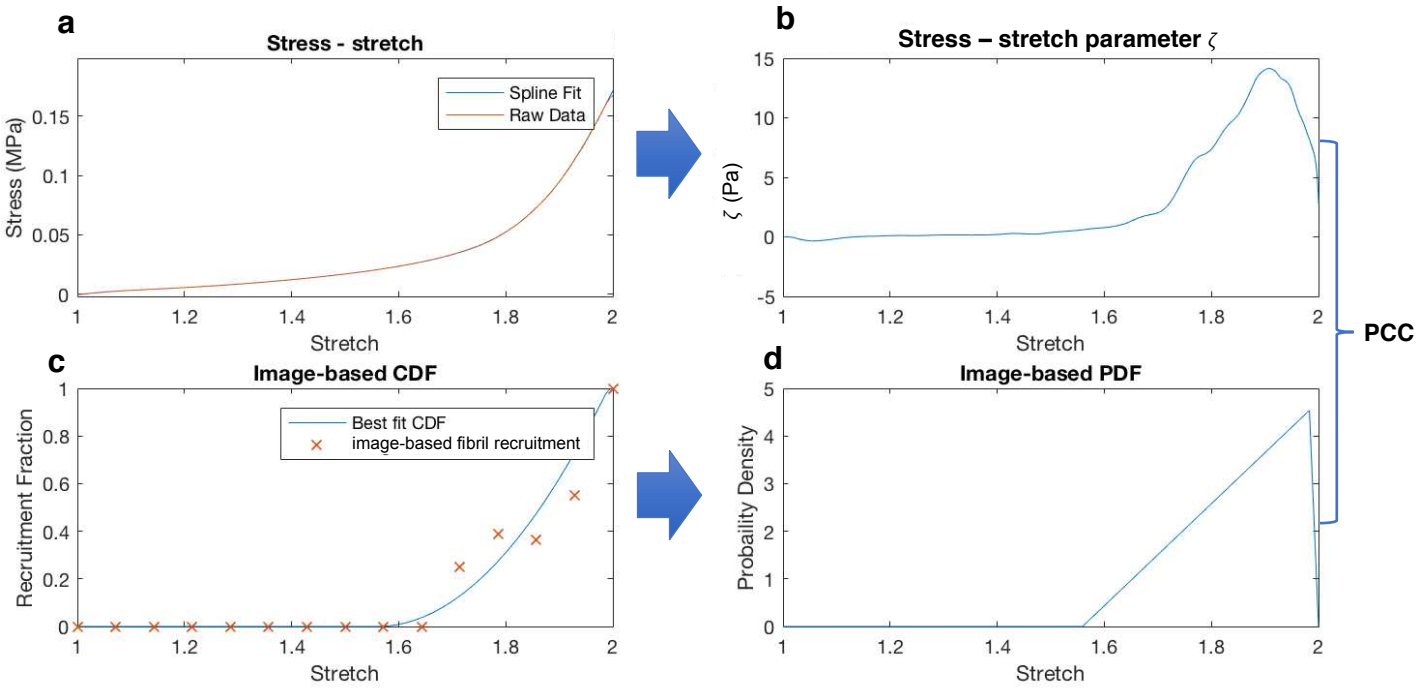


**Figure 3.a** Exemplary artery stress-stretch curve, spline fitted. **b** Stress-stretch parameter $\zeta$. **c** Image-based fibril recruitment and best-fit CDF for $S_c = S_c^*$. **d** corresponding PDF. PCC calculated for **b** compared with **d**.

**Figure 4**
**Click here to download Figure: Fig4.docx**

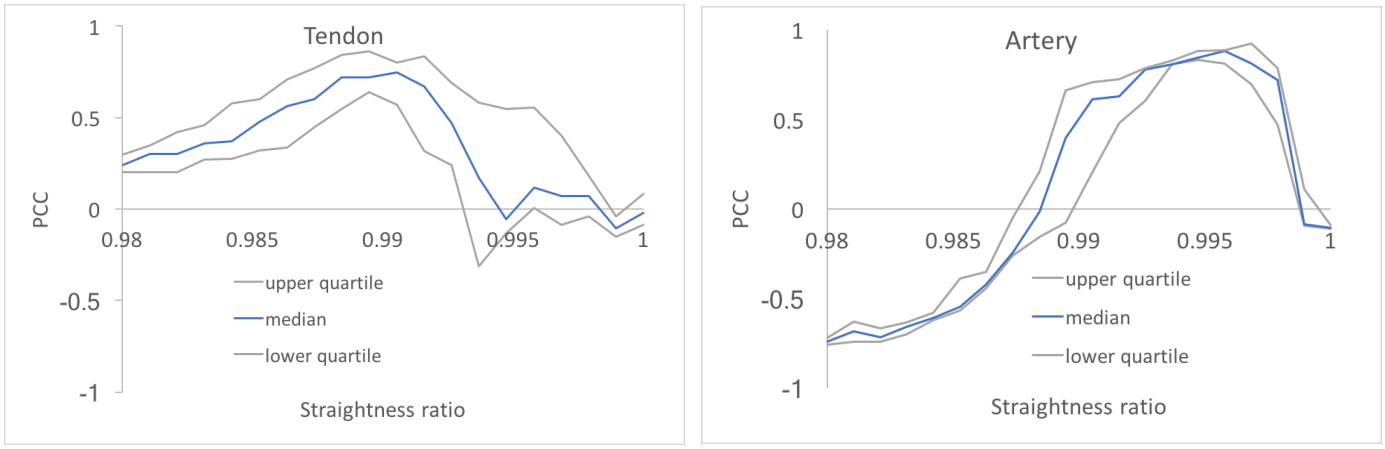


**Figure 4.** Variation of Pearson Correlation Coefficient with straightness ratio for tendon (n=7) and artery (n=5).

Conflict of interest statement

Not one of the authors is aware of any financial or personal relationships with other people or organisations that could inappropriately influence (bias) their work.